Remote Sensing of Environment xxx (2011) xxx–xxx

Contents lists available at ScienceDirect

Remote Sensing of Environment

journal homepage: www.elsevier.com/locate/rse

Validation of AMSR-E soil moisture using L-band airborne radiometer data from National Airborne Field Experiment 2006

Iliana Mladenova [a,f,*], Venkat Lakshmi [a], Thomas J. Jackson [b], Jeffrey P. Walker [c,g], Olivier Merlin [c,d], Richard A.M. de Jeu [e]

[a] Department of Geological Sciences, University of South Carolina, Columbia, SC, USA
[b] Hydrology and Remote Sensing Lab, USDA, Beltsville, MD, USA
[c] Department of Civil and Environmental Engineering, University of Melbourne, Melbourne, Victoria, Australia
[d] Centre d'Etudes Spatieles de la BIOsphere, Toulouse, France
[e] Department of Hydrology and GeoEnvironmetal Sciences, Vrije Universiteit, Amsterdam, The Netherlands
[f] USDA-ARS, Hydrology and Remote Sensing Lab BARC-West, B007, 10300 Baltimore Ave. Beltsville, MD 20705, USA
[g] Monash University, Department of Civil Engineering, Melbourne, Victoria, Australia

ARTICLE INFO

Article history:
Received 13 June 2009
Received in revised form 30 March 2011
Accepted 2 April 2011
Available online xxxx

Keywords:
Algorithm validation
AMSR-E
Irrigation
L-band radiometry
NAFE
Rice paddies
Standing water

ABSTRACT

AMSR-E has been extensively evaluated under a wide range of ground and climate conditions using *in situ* and aircraft data, where the latter were primarily used for assessing the T_B calibration accuracy. However, none of the previous work evaluates AMSR-E performance under the conditions of flood irrigation or other forms of standing water. Also, it should be mentioned that global soil moisture retrievals from AMSR-E typically utilize X-band data. Here, C-band based AMSR-E soil moisture estimates are evaluated using 1 km resolution retrievals derived from L-band aircraft data collected during the National Airborne Field Experiment (NAFE'06) field campaign in November 2006. NAFE'06 was conducted in the Murrumbidgee catchment area in southeastern Australia, which offers diverse ground conditions, including extensive areas with dryland, irrigation, and rice fields. The data allowed us to examine the impact of irrigation and standing water on the accuracy of satellite-derived soil moisture estimates from AMSR-E using passive microwave remote sensing. It was expected that in fields with standing water, the satellite estimates would have a lower accuracy as compared to soil moisture values over the rest of the domain. Results showed sensitivity of the AMSR-E to changes in soil moisture caused by both precipitation and irrigation, as well as good spatial (average $R = 0.92$ and $RMSD = 0.049$ m^3/m^3) and temporal ($R = 0.94$ and $RMSD = 0.04$ m^3/m^3) agreement between the satellite and aircraft soil moisture retrievals; however, under the NAFE'06 ground conditions, the satellite retrievals consistently overestimated the soil moisture conditions compared to the aircraft.

Published by Elsevier Inc.

1. Introduction

It has been demonstrated that the assimilation of soil moisture observations in hydrologic models can improve the accuracy of hydrologic prediction, including evaporation, surface temperature, and root-zone soil moisture (Ni-Meister et al., 2006). Station observations of soil moisture satisfy the temporal requirements of modeling; however, the point-based nature of these measurements combined with the limited number of well-established long-term soil moisture networks in the world restricts their use. Considering the dynamic nature of the soil moisture and the strong heterogeneous character of the Earth surface, point-based monitoring alone might not be sufficient to fully capture the spatial variability without additional efforts, such as those described by Cosh et al. (2004). An alternative is to use the more extensive, but shallower and less frequent, soil moisture monitoring from satellite microwave remote sensing.

Soil moisture retrievals from the European Space Agency (ESA) Soil Moisture and Ocean Salinity (SMOS) mission, and the National Aeronautics and Space Administration (NASA) Soil Moisture Active Passive (SMAP) mission, to be launched in 2014, are highly anticipated since both missions are designed to operate at 1.4 GHz (L-band) that is optimal for soil moisture monitoring. Although it was not originally planned for soil moisture mapping, the Advanced Microwave Scanning Radiometer (AMSR-E) on the NASA's Aqua platform was the most suitable sensor system prior to the launch of SMOS in November of 2009. AMSR-E operates in six channels ranging between 6.9 GHz and 89.0 GHz, and provides global surface soil moisture estimates in near-real time every one to three days, from 2002 to the present. A summary of the relevant to this research technical specifications of AMSR-E is provided in Table 1.

AMSR-E has been extensively studied to determine its accuracy across a wide range of ground and climatological conditions using both

* Corresponding author at: USDA-ARS, Hydrology and Remote Sensing Lab BARC-West, B007, 10300 Baltimore Ave. Beltsville, MD 20705, USA. Tel.: +1 (301) 504 9109.
E-mail address: Iliana.Mladenova@ARS.USDA.GOV (I. Mladenova).

0034-4257/$ – see front matter. Published by Elsevier Inc.
doi:10.1016/j.rse.2011.04.011

Table 1
PLMR/L-MEB–AMSR-E/LPMR comparison table.

Product	PLMR SM (Merlin et al., 2008)	AMSR-E
Relevant instrument specifications		
Frequency	L-band (1.413 GHz),	C-band (6.6 GHz)
Polarization	Horizontal	Horizontal
Sp. resolution	1 km grid spacing	25 km grid spacing
Incidence angle	7º	55º
Model	L-MEB (Wigneron et al., 2007)	LPRM SM (de Jeu & Owe, 2003; Owe et al., 2001)
Assumptions		
	–Uniform footprint in terms of canopy and soil temperature. –Homogenous vegetation –$T_{canopy} = T_{soil}$	–Uniform footprint in terms of canopy and soil temperature. –Homogenous vegetation –$T_{canopy} = T_{soil}$ –Surface roughness effect – minimal –Canopy characteristics same for H- and V-pol
Formalism		
τ–ω model	Mo et al., 1982	Mo et al., 1982
Dielectric model	Dobson et al., 1985	Wang and Schmugge, 1980
Surface roughness effects	Wang & Choudhury, 1981	Wang & Choudhury, 1981
Soil effective temperature	Uses near-surface and deep soil temperature data (Wigneron et al., 2007)	Microwave polarization difference index computed using Ka-band (37 GHz) T_B data (de Jeu & Owe, 2003; Owe et al., 2001)
Vegetation effects	τ is parameterizes as a function of LAI (Wigneron et al., 2007)	Solves simultaneously for soil moisture and vegetation optical depth (de Jeu & Owe, 2003; Owe et al., 2001)
Contribution of standing water	Removed (Ulaby et al., 1981)	Ignored
Parameterization		
Vegetation parameter (b)	0.15[a]	–
Land classification/use	Site specific	–
Surface roughness characterization (H & Q)	$H = 0.1$[a] $Q = 0$[a]	$H = 0.09$ $Q = 0.115$
Single scattering albedo	0.05[a]	0.05
Soil properties	Site specific	FAO

[a] Values were determined using the default set of SMOS parameters for single-scattering albedo, surface roughness, vegetation parameter b.

airborne data collected during several soil moisture (SM) experiments (Bindlish et al., 2006, 2008; Jackson et al., 2004, 2005), *in situ* measurements (Bosch et al., 2006; Choi et al., 2008; Njoku et al., 2003; Shibata et al., 2003; Walker et al., 2003), and model outputs (Choi et al., 2008). Validation areas have primarily included well-instrumented watersheds throughout the continental US, Northern Mexico, Brazil, and various parts of Australia. However, none of these evaluation studies assessed AMSR-E retrieval accuracy under the conditions of flood irrigation or other forms of standing water. Moreover, the available aircraft data were primarily used for assessing AMSR-E brightness temperature (T_B) calibration accuracy (Bindlish et al., 2006, 2008; Jackson et al., 2004, 2005).

Although the lower microwave frequencies have been shown to be more sensitive to soil moisture (Jackson, 1993; Wang, 1987) due to the strong presence of radio frequency interference (RFI) in the C-band (6.925 GHz) over certain countries, the X-band (10.65 GHz) measured T_B data has been primarily used for global soil moisture retrieval (Njoku et al., 2003, 2005). This research evaluates a data set that utilizes C-band AMSR-E microwave brightness temperatures, which were incorporated in the multichannel-based Land Parameter Retrieval Model (LPRM) approach to obtain soil moisture estimates (Owe et al., 2001, 2008).

Thus, the main objectives of this study are to: i) assess the accuracy of the LPRM C-band derived soil moisture product, ii) evaluate the sensitivity to changes in soil wetness under the conditions of extensive irrigation, and iii) study the impact of standing water on the AMSR-E retrieval accuracy. We will address the outlined goals using the National Airborne Field Experiment 2006 (NAFE'06) aircraft soil moisture data set derived from the Polarimetric L-band Multibeam Radiometer (PLMR). Furthermore, the standing water (rice fields) present in the NAFE'06 domain located in the Murrumbidgee catchment area, southeastern Australia, affords the opportunity to understand its impact on the AMSR-E soil moisture accuracy. It is expected that the presence of irrigation and standing water in the region will challenge the accuracy of the examined products and may result in errors greater than the AMSR-E (SMOS and SMAP) specified retrieval accuracy of 0.04 m^3/m^3.

2. Soil moisture data sets

2.1. National Airborne Field Experiment 2006

The NAFE'06 field campaign was conducted between October 29th and November 20th 2006. *In situ* data collection was carried out across three domains: Yanco (3600 km^2), Kyeamba (600 km^2), and Yenda (0.26 km^2). All three sites are located in the Murrumbidgee catchment area and offer a wide range of vegetation, topographic and climatic conditions (Merlin et al., 2008). However, only the Yanco area had a sufficient number of aircraft data sets to support the analysis proposed here. The aircraft mapping extent and coverage in relation to the AMSR-E footprint are shown in Fig. 1. One-third of the domain (Fig. 1, western portion) falls within the Coleambally Irrigation Area (CIA). Irrigation typically occurs from October through mid-March. The predominant vegetation types in the CIA include rice, dry and irrigated wheat and pasture, fallow, and croplands, while the rest of the domain is mainly rangeland. During the month of November 2006 (NAFE'06 duration), rice paddies were flooded with around 30 cm of water. Walker et al. (2006) reported that by late October, the average coverage without any standing water drops typically from ~75% to ~15% and that as the percent submerged land increases, the measured T_B decreases significantly. This phenomenon can potentially introduce

Please cite this article as: Mladenova, I., et al., Validation of AMSR-E soil moisture using L-band airborne radiometer data from National Airborne Field Experiment 2006, *Remote Sensing of Environment* (2011), doi:10.1016/j.rse.2011.04.011

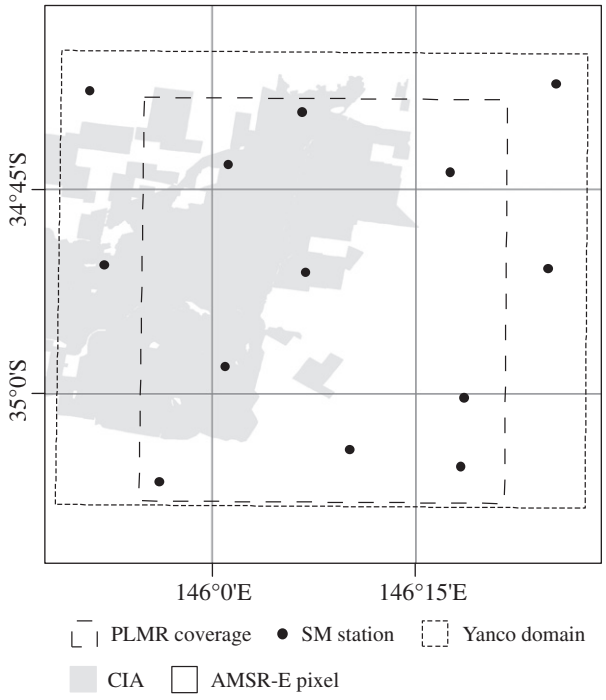

Fig. 1. A schematic representation of the NAFE'06 domain illustrating the location of the PLMR flight area (dashed line) in the Yanco region (dotted line), extent of the Coleambally irrigation area (CIA, grey polygon), AMSR-E pixel (solid line), and locations of the permanent soil moisture (SM) stations (black dots).

an error greater than 0.04 m^3/m^3 with as little as 2%–2.5% of the area flooded (Davenport et al., 2008; Walker et al., 2006).

Eleven regional aircraft soil moisture were derived from PLMR (see Table 1 for instrument characteristics). Additional data collected concurrently with the aircraft flights included *in situ* soil moisture readings of the top 6 cm of the soil profile measured over six farms at 250 m grid spacing, soil and vegetation samples. The later three were used to determine several parameters that are needed for the T_B-soil moisture inversion such as soil texture, canopy type, vegetation water content etc., and to assess the accuracy of the resulting soil moisture maps. The aircraft time window was scheduled to mimic the SMOS overpass time of 0600 am and occurred typically between 0800 am and 1030 am, except for November 13th and 14th, when the PLMR flight was done in the 1100 am to 1330 pm time span. The calibrated and gridded 1 km T_B data are available from the NAFE website.[1]

2.2. Soil moisture products

2.2.1. LPRM AMSR-E soil moisture product

The C- and X-band satellite observations from the AMSR-E radiometer are used to derive surface soil moisture. Level 2A global brightness temperatures are obtained from National Snow and Ice Data Center (NSIDC) with a spatial resolution of 56 km, and the retrieved soil moisture is resampled to a 0.25-degree grid in order to become spatially consistent. AMSR-E scans the Earth's surface in an ascending (1330) and descending (0130) mode. In this study, we used the observations from the ascending mode (Ashcroft & Wentz, 2003; NSIDC, 2006).

The brightness temperatures were converted to soil moisture values with the Land Parameter Retrieval Model (Owe et al., 2001, 2008). A brief summary of the model is provided in Table 1. The LPRM is based on a one layer microwave radiative transfer model (Mo et al., 1982) that links surface geophysical variables (e.g., soil moisture, vegetation water content, and soil/canopy temperature) to the observed brightness temperatures. The following assumptions are required: uniform landscape temperature (soil and canopy), homogeneous vegetation characteristics within the satellite footprint, all vegetation parameters are the same for H- and V-polarizations, and minimal surface roughness effects. Vegetation canopy and soil temperature were estimated with vertical polarized Ka-band observations (De Jeu & Owe, 2003) and the vegetation density or vegetation optical depth was derived simultaneously with the LPRM according to the analytical approach of Meesters et al. (2005).

The LPRM-derived product has been tested in a series of validation studies (e.g., De Jeu et al., 2008; Rüdiger et al., 2009; Wagner et al., 2007). Of particular interest for this work is the assessment of Draper et al. (2009), as it presents the evaluation results of the LPRM algorithm performance over Australia. The authors examined the temporal and spatial accuracy of the LPRM retrievals using *in situ*-measured soil moisture and precipitation over the Murrumbidgee catchment area. The results from the comparison analyses demonstrated strong agreement of the LPRM retrievals with the station soil moisture observations (correlation >0.8 and Root Means Square Difference ($RMSD$)<0.03 m^3/m^3) and adequate spatial correspondence with the precipitation maps.

Since no RFI was detected over Australia (Njoku et al., 2005) and based on comparison of the LPRM and NASA products (Draper et al., 2009) over the Murrumbidgee catchment area, the C-band LPRM product was used in this study.

2.2.2. L-MEB PLMR soil moisture product

T_B to soil moisture inversion for the PLMR data was performed using a modeling approach based on the τ–ω model and the proposed default SMOS values for surface roughness (H), single scattering albedo (ω), canopy (b), and polarization mixing (Q) parameters (Mo et al., 1982; Wigneron et al., 2007); see Table 1 for summary of the model. The accuracy of the derived estimates was assessed using field data collected over three of the six focus farms. Approximately 82% of the validation area were covered by non-irrigated vegetation types and the remaining 28% were occupied by irrigated crops. Results showed that the precision of the soil moisture estimates was strongly dependent on the existence or lack of irrigation in the sampling domain. The PLMR product was found to be well-correlated with the ground observed soil moisture values over the non-irrigated portion of the validation domain ($RMSE = 0.033$ m^3/m^3 and a bias of 0.004 m^3/m^3, where $RMSE$ is Root Mean Square Error). On the other hand, the areas covered by irrigated crops were associated with lower retrieval accuracy ($RMSE = 0.10$ m^3/m^3 with a bias of -0.093 m^3/m^3), where the large bias here was explained by a strong vertical gradient and/or increase in the dielectric roughness. A full description of the aircraft retrieval and validation using *in situ* SM are offered in Merlin et al. (2009).

2.3. Algorithms comparison and error sources

Some of the most important components of the extensive soil moisture campaigns are: i) evaluation of AMSR-E T_B calibration precision (Bindlish et al., 2006, 2008; Jackson et al., 2005), and ii) validation of existing, and development of new, retrieval algorithms and accuracy assessment of the corresponding soil moisture products. As previously noted (see Introduction), the available aircraft data were primarily used in studies focusing on T_B calibration accuracy. The main focus of our research is more closely related to the second of these two aspects. Therefore, in the remaining part of this section, we will provide a general overview of the nature of the microwave retrieval algorithms including a brief comparison of the L-MEB and the LPRM models (Table 1), as well as an overview of

[1] See: http://www.nafe.unimelb.edu.au/.

Please cite this article as: Mladenova, I., et al., Validation of AMSR-E soil moisture using L-band airborne radiometer data from National Airborne Field Experiment 2006, *Remote Sensing of Environment* (2011), doi:10.1016/j.rse.2011.04.011

potential error sources and of the possible/expected causes for discrepancies between the aircraft and the satellite product.

Passive soil moisture retrieval algorithms (Jackson, 1993; Owe et al., 2001) are based on the radiative transfer equation and include T_B correction for the effect of vegetation, surface roughness, and physical temperature. Most of the variables affecting the measured signal have different levels of impact at different frequencies and are both frequency and polarization dependent (e.g., vegetation attenuation is known to be smaller at lower frequencies and at horizontal polarization). There are several well-established algorithms (Jackson, 1993; Njoku et al., 2003; Owe et al., 2001; Wigneron et al., 2007) for T_B-soil moisture inversion. The strong ground surface heterogeneity and atmospheric forcing, along with the shallow penetration depth of the microwaves, result in dynamic temporal and spatial variability of the near surface soil moisture. This underscores the efforts for improvement of the existing methodologies despite their demonstrated high retrieval accuracy. For example, Walker et al. (2003) emphasize that none of the available retrieval algorithms account for the effect of exposed rocks, which may have a strong effect on the surface roughness and, as observed by Bindlish et al. (2008), can result in higher than the actual T_B, consequently leading to erroneous estimates of soil moisture.

Detailed comparison between the LPMR and the L-MEB algorithms in terms of methodology, assumptions, and parameterization is given in Table 1. Although based on the same principles (τ–ω model), the LPRM and the L-MEB algorithms utilize different approaches in the estimation of vegetation optical depth, and soil and canopy temperature (Wagner et al., 2007). Furthermore, differences in assumptions and techniques for reducing the T_B dependence on surface temperature can generate differences between the retrieved soil moisture products. Also, the satellite-aircraft soil moisture comparisons proposed here involve different wavelengths. Wavelength characteristics of the remote sensing systems are particularly important because they determine the thickness of the contributing layer. The aircraft instrument operates at a lower frequency, (L-band); therefore, the AMSR-E (C-band) sensor in this case will be associated with the shallower penetration depth. These two factors, along with the use of straightforward spatial averaging of the aircraft retrievals within the satellite footprint, introduce the possibility of differences in the final soil moisture estimates (McCabe et al., 2005).

LPRM is a multichannel dual polarization type of approach; thus, two additional sources of error should be accounted for: the difference in footprint size at the different frequencies, and calibration accuracy of the two polarizations employed in the soil moisture retrieval (Njoku & Chan, 2006). It is important that the two channels are properly co-located and re-gridded to the same spatial resolution so that it can be assumed that they observe the same ground area at the same time. Most importantly, when retrieving AMSR-E, the algorithms (incl. LPRM) are parameterized at a global scale, often use fixed values for certain factors (e.g., roughness and single scattering albedo), and utilize non-comprehensive very coarse resolution ancillary sources (e.g., soil texture maps) as compared to the aircraft retrieval, where detailed site-specific model inputs are typically available. This consequently leads to more accurate aircraft estimates.

3. Results and Discussion

The temporal and spatial soil moisture variability over the NAFE'06 area is mostly controlled by the temporal and spatial distribution of rainfall: amount, intensity, and occurrence. Under the low vegetation cover conditions in the NAFE'06 domain, the volumetric soil moisture content of the top soil layer is primarily a function of infiltration and evaporation (Teuling et al., 2007). There were 2 major precipitation events during NAFE'06, occurring on November 3rd and 13th. These resulted in ~6 mm and 11 mm of rainfall respectively. Based on the spatial variability in the PLMR and station soil moisture data, it appeared that both precipitation events were homogenously distributed throughout the area. The 1st precipitation event occurred after a month-long period of almost no precipitation. Therefore, it was expected that both sensor systems would exhibit a noticeable increase in soil moisture. This was confirmed by the greater daily mean and maximum values on November 04th and 13th respectively (see Table 2). Although the general temporal trend of wetting and drying (Fig. 3) is similar for both sensors, the AMSR-E data show a smaller response to the first storm and a smaller change in mean moisture as compared to PLMR ($AMSR\text{-}E_{Nov04-Oct31}$ SM Change = 0.01 m^3/m^3 vs. $PLMR_{Nov04-Oct31}$ SM Change = 0.06 m^3/m^3). This can be attributed in part to the fact the AMSR-E's overpass is later in the day as compared to the PLMR. The shallower AMSR-E sensing depth (~2 cm in C- vs. ~5 cm in L-band), fast infiltration, and rapid evaporation rates after the extensive drought, enhanced by the warm surface and air temperatures, could explain the observed differences. This effect was not observed on November 13th because of the minor rainfall event that occurred on November 12th. Moreover, the measured air (Griffith Meteorological Station) and surface temperatures (MODIS daily LST product) were lower on this day, with an average of 4 °C at the time of the second rainfall event. Under these cooler and wetter soil moisture conditions, the mean AMSR-E and PLMR soil moisture retrievals were expected to be closer, resulting in a lower *RMSD* and higher correlation coefficients. The overall mean temporal correlation coefficient (R) and *RMSD* estimated using the average daily AMSR-E and PLMR soil moisture values (NAFE'06 duration) were 0.94 and 0.04 m^3/m^3 respectively, demonstrating good temporal agreement between the AMSR-E- and PLMR-derived soil moisture products.

Mean comparisons of SM on a daily basis (Fig. 3) showed a wet AMSR-E bias that was largest in the lower soil moisture range (up to ~0.11 m^3/m^3) for the duration of the campaign (AMSR-E coverage on November 2nd was limited; therefore, that day was excluded from the analyses). The opposite was reported by McCabe et al. (2005) when comparing AMSR-E (X-band; operational product) and PSR (C-band; Land Surface Microwave Emission Model retrieval) soil moisture products over dense agricultural vegetation. Another important similarity between the AMSR-E and PLMR SM time series is the rapid drying trend after rainfall events. This tendency is more noticeable in the AMSR-E product. Due to the difference in sensing depth (approximately $^1/_4$ to $^1/_{10}$ of the wave length) between AMSR-E and an aircraft-derived product, AMSR-E should have a shallower sensing depth. As a result, it is expected that the satellite-derived SM product would exhibit a larger soil moisture dynamic range and result in underestimation of SM for dry conditions and overestimation on wet days as compared to the aircraft estimates. This tendency observed by McCabe et al. (2005) was not evident in NAFE'06. Describing NAFE'06 statistics within the context of the results presented in McCabe et al. (2005) will be difficult due to differences in retrieval algorithms, frequencies, canopy cover, surface, and RFI conditions. Therefore, no generalizations will be carried out.

The spatial distribution of the temporal coefficients between AMSR-E and PLMR SM (averaged to 25 km ground spacing) is shown in Fig. 4. The analysis indicated similar AMSR-E and PLMR performance ($R_{average} = 0.92$ and $RMSD_{average} = 0.05$ m^3/m^3, based on 9 corresponding pixels and 7 coincident days). Both sensors adequately depicted the irrigation area to be wetter and to have less soil moisture variability than the rest of the domain due to the controlled water input. AMSR-E SM estimates were greater as compared to the PLMR-derived product.

From analysis of the PLMR SM images (Fig. 2, 1st row) in the context of land surface features encountered in the area and the precipitation amount received during the campaign, the following observations can be made: (1) There is significant sensitivity to changes in wetness conditions that is evident in the wetting and drying patterns; (2) The CIA generally exhibits wetter conditions than the rest of the domain; and (3) Portions of the irrigation area maintain a relatively constant high soil moisture level. For example, most of the

Please cite this article as: Mladenova, I., et al., Validation of AMSR-E soil moisture using L-band airborne radiometer data from National Airborne Field Experiment 2006, *Remote Sensing of Environment* (2011), doi:10.1016/j.rse.2011.04.011

Table 2
Daily statistics describing the AMSR-E and PLMR soil moisture variability over the regional flight box.

Date		31-Oct	4-Nov	7-Nov	9-Nov	13-Nov	14-Nov	16-Nov
RMSD [m^3/m^3]		0.07	0.03	0.06	0.08	0.03	0.03	0.04
R		0.31	0.15	0.53	0.44	0.43	0.50	0.67
Average	PLMR	0.04	0.10	0.04	0.04	0.19	0.11	0.10
	AMSR-E	0.11	0.12	0.10	0.11	0.21	0.14	0.13
Minimum	PLMR	0.02	0.08	0.02	0.02	0.17	0.09	0.07
	AMSR-E	0.10	0.11	0.07	0.10	0.20	0.13	0.12
Maximum	PLMR	0.10	0.15	0.09	0.08	0.26	0.14	0.15
	AMSR-E	0.13	0.14	0.12	0.13	0.21	0.14	0.14
Standard deviation	PLMR	0.022	0.024	0.021	0.020	0.027	0.020	0.026
	AMSR-E	0.012	0.012	0.014	0.009	0.006	0.006	0.006
Coefficient of variance [%]	PLMR	49.09	23.01	49.78	50.88	14.43	18.32	26.24
	AMSR-E	11.05	9.92	14.68	7.89	2.92	4.68	4.95

NOTE:
The correlation coefficient (*R*), *RMSD*, Standard Deviation (*St. Dev.*), and coefficient of variance (*CoV*) were computed using all coincident pixels between the two soil moisture products on a daily basis.

pixels with SM values greater than ~0.20 m^3/m^3 in the CIA were classified as rice fields based on the comparison with Landsat-derived vegetation classification map of the area developed by Cosh et al., (under revision); (4) The lake in the mid-northern part of the domain is clearly visible in all the PLMR images; and, (5) The small localized rainfall event on November 16th in the southwest corner of the domain with a northeast orientation is apparent in the PLMR coverage from that day. These observations further demonstrate the capability of the PLMR to adequately represent change in moisture conditions in the area.

The daily spatial AMSR-E soil moisture images for the NAFE'06 duration are presented in Fig. 2, 2nd row. One would expect to see an increase in SM following the two rainfall events (November 3rd and 13th) followed by dry down periods. No AMSR-E data were available for the time of the 1st rainfall event. The 2nd rainfall event is characterized by a large increase in the SM values on November 13th with ~0.1 m^3/m^3 and 0.15 m^3/m^3 for AMSR-E and PLMR respectively. The following similarities between the AMSR-E and PLMR (Fig. 2) SM maps can be observed: wetting and drying trends, adequate response to precipitation, and generally wetter conditions in the western part of the domain. Under dry conditions at the 25 km AMSR-E pixel size, the CIA and presence of standing water are shown to be less prominent as compared to the PLMR images. Lower AMSR-E soil moisture sensitivity compared to PLMR is evident in all days; however, as expected under dry soil moisture conditions, the AMSR-E shows an increase in spatial variability as a result of the enhanced difference in soil moisture between the irrigated and non-irrigated parts of the domain (when dry, the AMSR-E range across the study domain varies between 0.03 $m^3/m^3$and 0.05 m^3/m^3 as compared to 0.01 m^3/m^3 under wet soil moisture conditions).

Overall AMSR-E soil moisture is higher and has a narrower dynamic range and lower variability (Table 2). This is evident in the standard deviation (*St. Dev.*) and coefficient of variance (*CoV*) (average PLMR *St. Dev.* is 0.023 m^3/m^3 vs. only 0.009 m^3/m^3 for AMSR-E, and the average *CoV* for PLMR is about 33% vs. 8% for AMSR-E). The daily spatial correlation coefficients are lower than the overall mean *R* due to the low daily sensitivity range [Mean AMSR-E Daily *Range* = 0.02 m^3/m^3 (0.06 $m^3/m^3$for PLMR SM) vs. AMSR-E *Range* for NAFE'06 duration = 0.14 m^3/m^3 (0.24 $m^3/m^3$for PLMR SM)]. On days with very dry soil moisture conditions (i.e. October 31st, November 7th and 9th), the error difference estimates were higher (*RMSD* = 0.07 m^3/m^3, 0.06 m^3/m^3 and 0.08 m^3/m^3 respectively). For these three dates, the

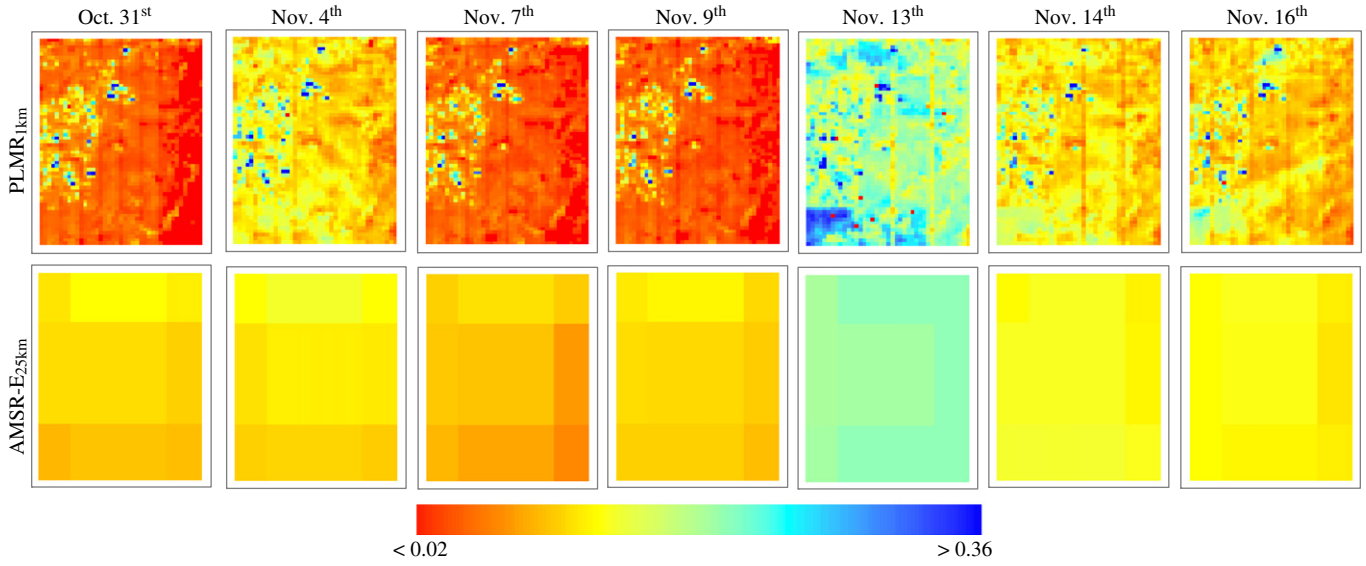

Fig. 2. PLMR- and AMSR-E-derived soil moisture [m^3/m^3] products at 1 km and 25 km spatial resolution respectively over the Yanco region during the NAFE'06 field campaign.

Please cite this article as: Mladenova, I., et al., Validation of AMSR-E soil moisture using L-band airborne radiometer data from National Airborne Field Experiment 2006, *Remote Sensing of Environment* (2011), doi:10.1016/j.rse.2011.04.011

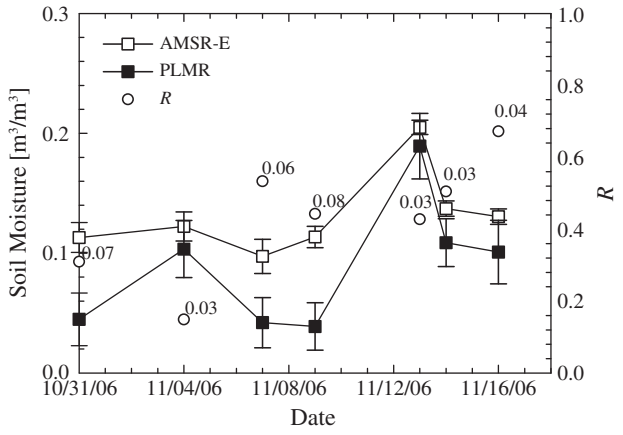

Fig. 3. Daily variation of AMSR-E (C-band, Asc.) and PLMR (aggregated to AMSR-E pixel size) soil moisture (SM) products at 0.25° resolution over the regional flight box (see Fig. 1) for the duration of the NAFE'06 field campaign. Bars show ± 1 standard deviation, and the number next to the *R*-value in the plot is the *RMSD* for that particular day.

AMSR-E strongly overestimated the soil moisture as compared to PLMR (average PLMR = 0.04 m^3/m^3 vs. AMSR-E = 0.10 m^3/m^3). Under wet conditions, both products appear to be better correlated than when dry ($R_{Oct31} = 0.31$ and $RMSD_{Oct31} = 0.07$ m^3/m^3; $R_{Nov13} = 0.43$ and $RMSD_{Nov13} = 0.03$ m^3/m^3) with similar mean soil moisture (Fig. 3). The observed difference on a daily basis between the satellite and the aircraft estimates was consistent with and within similar range as the one reported by Davenport et al. (2008). Thus, it can be concluded that the higher soil moisture tendency observed in AMSR-E and evident from both the temporal and spatial analyses (Fig. 4 and Table 2) is minimal when wettest and it increases as drying occurs (i.e., October 31st, November 9th).

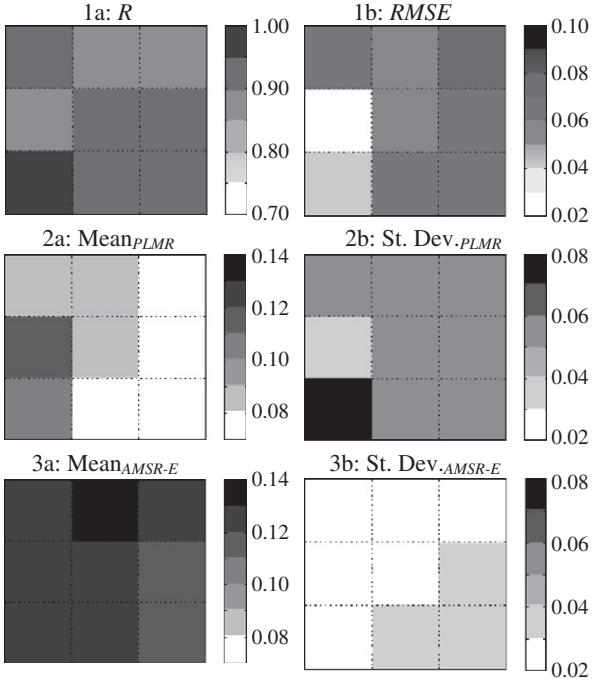

Fig. 4. Spatial distribution of Pearson Correlation Coefficient (*R*) and *RMSD* between PLMR and AMSR-E at 0.25° resolution over the NAFE'06 study domain (i.e. regional flight box, see Fig. 1). The plots were built using all coincident days between the two sensors.

Along with the rapid increase in standing water in the rice paddies, by the end of October/early November, the CIA area (Fig. 1) becomes subject to extensive irrigation. Assuming that on non-rainy days the most significant cause for soil moisture change over the area (Fig. 5) will be due to the water input to the system by irrigation, one can expect less variability during dry days over the non-irrigated part of the domain. This pattern is clearly visible in the October 19th–November 2nd dry period. In order to illustrate the SM variability preceding the irrigation season, we extended the analysis period by including the whole month of September 2006. Under low soil moisture conditions and prior to the irrigation season, the irrigated and non-irrigated portions exhibited similar behavior to rainfall events. This can be seen for September 5th and 6th, when the soil moisture changes in the two portions of the domain were almost the same. A similar response after the beginning of the irrigation around November 14th was due to the increase in soil moisture content after the November 13th rainfall event, when the two portions appeared to be equally wet (Fig. 2). After the beginning of the irrigation period, a rainfall event would result in a more significant change for the dry area than the irrigated portion. Similar behavior can be observed around October 16th.

Before discussing further the results, it should also be noted that the impact of water was removed in the PLMR retrieval (Merlin et al., 2009). Applying the same approach as presented in Walker et al. (2006), the percent of rice field coverage at 25 km was determined based on a simple threshold classification methodology, where a pixel was classified as standing water if the surface reflectance of Landsat band 5 was less than 0.15. At the AMSR-E scale, using a Landsat scene acquired on November 7th, it was estimated that one-third of the domain had rice field coverage greater than 1% and only one-ninth greater than 4% (with an average of ~2% over the irrigated part of the NAFE'06 domain). As noted earlier even as little as 2.5% of standing water could result in retrieval error greater than 0.04 m^3/m^3 based on the 1 km scale (coarse resolution) analysis (Davenport et al., 2008 and Walker et al., 2006). Thus, it was expected that in fields with standing water the satellite retrieval algorithm would have a lower accuracy as compared to the rest of the domain. It should be noted that in this case the pixels that have standing water are also part of the Coleambally Irrigation area. Thus, along with the standing water, the soils in the CIA will be close to saturation (if irrigation occurs). Both products were better correlated over the non-irrigated portion with an *R* of 0.93 as compared to the irrigated where the correlation coefficient was 0.84. Error analysis was consistent with the correlation values indicating lower accuracy over the irrigated half [0.3 m^3/m^3 (irrigated) vs. 0.02 m^3/m^3 (non-irrigated)].

Several factors could explain the observed difference: canopy cover, soil properties, and soil geometric roughness (e.g. LPRM model parameterization), presence of standing water and irrigation. Vegetation was very low (LAI between 0.4 and 0.8, Merlin et al., 2009) and the optical depth appear to be relatively homogenous at 25 km. Thus, the resulting canopy related error is negligible compared to the overall error (Davenport et al., 2008 and Merlin et al., 2009). Soil texture in terms of percent sand and clay fraction are needed for the dielectric mixing model which relates the dielectric constant to the soil emissivity. Merlin et al. (2009) demonstrated that even if the highest measured sand and clay fractions were utilized in the retrieval, the *RMSD* between the two runs (mean vs. maximum sand/clay values) was much smaller compared to the overall observed bias. Inaccurate surface roughness parameterization can impact the soil reflectivity, which in turn is related to the soil emissivity through the Kirchhoff's theorem. Under the NAFE'06 conditions, Merlin et al. (2009) reported that there was no significant difference in terms of surface roughness between the irrigated and the non-irrigated portions of the domain. Furthermore, after analyzing the surface roughness effect on the soil moisture derived using the τ–ω model, Davenport et al. (2008) concluded that for a single-angle system the surface roughness has a negligible impact on the retrieval error. Also,

Please cite this article as: Mladenova, I., et al., Validation of AMSR-E soil moisture using L-band airborne radiometer data from National Airborne Field Experiment 2006, *Remote Sensing of Environment* (2011), doi:10.1016/j.rse.2011.04.011

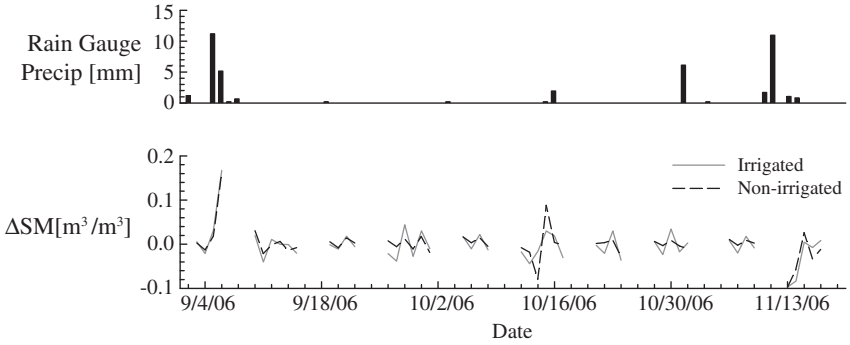

Fig. 5. Temporal change in AMSR-E soil moisture [m^3/m^3] over irrigated (solid line) and non-irrigated area (dashed line) and rain gauge precipitation measured in millimeters for the September 1st through November 30th, 2006 time period.

the same authors summarized that the largest likely errors caused by vegetation, surface roughness, and soil moisture variability within the coarse resolution radiometer footprint are insignificant (0.005, 0.002, and 0.005 m^3/m^3 respectively) compared to the error caused by not or inaccurately accounting for the effect of open water (0.10 m^3/m^3). The latter two factors listed in the beginning of this paragraph, standing water and irrigation, would cause the soil moisture content to be very high (e.g. great portion of the soils within the AMSR-E footprint are fully saturated or close to saturation). It is well known that there is a large difference between the dielectric constants of water (~80, i.e. rice paddies in the NAFE'06 case) and soil-water mixture (between ~4 and ~40 for dry and wet soils respectively). As it is evident, this contrast is most profound in the dry soil moisture range. If we assume that 5% of the footprint are flooded and the remaining 95% are very dry (i.e. no rainfall or irrigation) the weighted average dielectric constant for the footprint will ~8, which is 100% higher than the dielectric constant of the 95% of the footprint. Thus, both standing water and irrigation may consequently result in erroneous estimation of the overall footprint microwave emission and consequently offer a logical reason explaining the observed difference between the two soil moisture products under the NAFE'06 ground conditions.

4. Conclusions

C-band LPRM AMSR-E soil moisture product (Owe et al., 2001, 2008) was evaluated over an area with extensive irrigation and rice fields using the L-band PLMR-derived soil moisture product. Temporal and spatial analyses indicated good agreement under the NAFE'06 surface conditions for the duration of the campaign ($R_{spatial} = 0.92$ and $R_{temporal} = 0.94$, $RMSD_{spatial} = 0.05$ m^3/m^3 and $RMSD_{temporal} = 0.04$ m^3/m^3). Considering the retrieval algorithm and frequency differences, as well as differences in the time of observation and spatial resolution of the two sensors, this is better than expected. The irrigation area was indicated as the wettest part of the domain by both the AMSR-E and PLMR. The space-borne SM estimates were consistently greater than the air-borne derived soil moisture values showing the lowest *RMSD* when wetter (i.e. after precipitation). The difference between the AMSR-E and the PLMR SM products was greater at soil moisture values <~0.11 m^3/m^3.

Changes in AMSR-E soil moisture were evaluated over the irrigated and non-irrigated portions of the domain over a three-month period (September 1st through November 30th). Prior to the irrigation season, the behavior of soil moisture change in the two portions was similar, as expected. During the irrigation season, the non-irrigated portion of the domain exhibited more rapid increases and decreases in soil moisture resulting from precipitation and lower changes in SM on dry days as compared to the more moderate responses to rainfall and greater variability over the irrigated part of the domain.

Based on previous research (Davenport et al., 2008; Walker et al., 2006), the retrieval error was calculated to be ~0.04 m^3/m^3 at only as little as 2.5% of standing water [using 1 km (coarse) T_B data]. The irrigation portion of the NAFE'06 area presented with an average rice coverage of 2%. It was found that under the described ground conditions, AMSR-E overestimated the soil moisture content compared to PLMR on average by approximately 0.04 m^3/m^3 and the two products agreed better over the non-irrigated portion of the domain ($R_{IRR} = 0.83$ vs. $R_{NON\text{-}IRR} = 0.93$). Thus, the presence of standing water and irrigation might explain the observed difference between the AMSR-E and the PLMR under the ground conditions encountered in the NAFE'06 domain.

References

Ashcroft, P., & Wentz, F. (2003). *AMSR-E/Aqua L2A Global Swath Spatially-Resampled Brightness Temperatures (Tb) V001, September to October 2003.* Digital media. Boulder, CO, USA: National Snow and Ice Data Center (Updated daily).

Bindlish, R., Jackson, T. J., Gasiewski, A. J., Klein, M., & Njoku, E. G. (2006). Soil moisture mapping and AMSR-E validation using the PSR is SMEX02. *Remote Sensing of the Environment*, *103*(2), 127–139.

Bindlish, R., Jackson, T. J., Gasiewski, A., Stankov, B., Klein, M., Cosh, M. H., Mladenova, I., Watts, C., Vivoni, E., Lakshmi, V., Bolten, J., & Keefer, T. (2008). Aircraft based soil moisture retrievals under mixed vegetation and topographic conditions. *Remote Sensing of the Environment*, *112*(2), 375–390.

Bosch, D. D., Lakshmi, V., Jackson, T. J., Choid, M., & Jacobs, J. M. (2006). Large scale measurements of soil moisture for validation of remotely sensed data: Georgia soil moisture experiment of 2003. *Journal of Hydrology*, *323*, 120–137.

Choi, M., Jackobs, J. M., & Bosh, D. D. (2008). Remote sensing observatory validation of surface soil moisture using the Advanced Microwave Scanning Radiometer E, Common Land Model, and ground based data: Case study in SMEX03 Little River Region, Georgia, U.S. *Water Resources Research*, *44*, W08421.

Cosh, M. H., Jackson, T. J., Bindlish, R., & Prueger, J. H. (2004). Watershed scale temporal persistence of soil moisture and its role in validation satellite estimates. *Remote Sensing of Environment*, *92*(4), 427–435.

Cosh, M., O'Neill, P., McKee, L., Tao, J., & Jackson, T. (under revision). Land Cover Classification in a Diverse Agricultural Landscape: the National Airborne Field Experiment. *IEEE Geoscience and Remote Sensing Letters*.

Davenport, I. J., Melody, J., & Gurney, J. R. (2008). The effects of scene heterogeneity on soil moisture retrieval from passive microwave data. *Advances in Water Resources*, *31*, 1494–1502.

De Jeu, R. A. M., & Owe, M. (2003). Further validation of a new methodology for surface moisture and vegetation optical depth retrieval. *International Journal of Remote Sensing*, *24*(22), 4559–4578.

De Jeu, R. A. M., Wagner, W., Holmes, T., Dolman, A. J., Van de Giesen, N., & Friesen, J. (2008). Global soil moisture patterns observed by space borne microwave radiometers and scatterometers. *Surveys in Geophysics*, *29*(4–5), 399–420.

Dobson, M. C., ULaby, F. T., Hallikainen, M. T., & El-Rayes, M. A. (1985). Microwave dielectric behavior on wet soils, II, Dielectric mixing models. *IEEE Transactions on Geoscience and Remote Sensing*, *23*, 35–46.

Draper, C., Walker, J. P., Steinle, P. J., De Jeu, R. A. M., & Holmes, T. R. H. (2009). An evaluation of AMSR-E derived soil moisture over Australia. *Remote Sensing of Environment*, *113*(4), 703–710.

Jackson, T. J. (1993). Measuring surface soil moisture using passive microwave remote sensing. *Hydrological Processes*, *7*, 139–152.

Jackson, T. J., Bindlish, R., Gasiewski, A. J., Stankov, B., Klein, M., Njoku, E. G., Bosch, D., Coleman, T. L., Laymon, C. A., & Starks, P. (2005). Polarimetric Scanning Radiometer C- and X-Band microwave observations during SMEX03. *IEEE Transactions on Geoscience and Remote Sensing*, *43*(11), 2418–2430.

Please cite this article as: Mladenova, I., et al., Validation of AMSR-E soil moisture using L-band airborne radiometer data from National Airborne Field Experiment 2006, *Remote Sensing of Environment* (2011), doi:10.1016/j.rse.2011.04.011

Jackson, T. J., Hurkmans, R., Hsu, A., & Cosh, M. H. (2004). Soil moisture algorithm validation using data from the Advanced Microwave Scanning Radiometer (AMSR-E) in Mongolia. *Italian Journal of Remote Sensing*, *30*, 37–50.

McCabe, M. F., Gao, H., & Wood, E. F. (2005). Evaluation of AMSR-E derived soil moisture retrieved using ground-based and PSR airborne data during SMEX02. *Journal of Hydrometeorology*, *6*(6), 864–877.

Meesters, A. C. A., De Jeu, R. A. M., & Owe, M. (2005). Analytical derivation of the vegetation optical depth from the microwave polarization difference index. *IEEE Geoscience and Remote Sensing Letters*, *2*(2), 121–123.

Merlin, O., Walker, J. P., Kalma, J. D., Kim, E., Hacker, J., Panciera, R., Young, R., Summerell, G., Hornbuckle, J., Hafeez, M., & Jackson, T. J. (2008). The NAFE'06 data set: towards soil moisture retrieval at intermediate resolution. *Advances in Water Resources*, *31*(11), 1444–1455.

Merlin, O., Walker, J. P., Panciera, R., Escorihuela, M. J., & Jackson, T. J. (2009). Assessing the SMOS soil moisture retrieval parameters with high-resolution NAFE'06 data. *IEEE Geoscience and Remote Sensing Letters*, *6*(4), 635–639.

Mo, T., Choudhury, B. J., Schmugge, T. J., & Jackson, T. J. (1982). A model for microwave emission from vegetation-covered fields. *Journal of Hydrology*, *184*, 101–129.

Ni-Meister, W., Houser, P. R., & Walker, J. P. (2006). Soil moisture initialization for climate prediction: assimilation of scaling multifrequency microwave radiometer soil moisture data into a land surface model. *Journal of Geophysical Research*, *111* (D20102). doi:10.1029/2006JD007190.

Njoku, E. G., Ashcroft, P., Chan, T. K., & Li, L. (2005). Global survey and statistics of radio frequency interference in AMSR-E land observations. *IEEE Transactions on Geoscience and Remote Sensing*, *43*(5), 938–947.

Njoku, G., & Chan, S. K. (2006). Vegetation and surface roughness effects on AMSR-E land observations. *Remote Sensing of the Environment*, *100*(2), 190–199.

Njoku, E. G., Jackson, T. J., Lakshmi, V., Chan, T. K., & Nghiem, S. V. (2003). Soil moisture retrieval from AMSR-E. *IEEE Transactions on Geoscience and Remote Sensing*, *41*(2), 215–229.

NSIDC (2006). *Data Products and Services.* Boulder, CO: National Snow and Ice Data Center.

Owe, M., De Jeu, R. A. M., & Holmes, T. R. H. (2008). Multi-sensor historical climatology of satellite derived global land surface moisture. *Journal of Geophysical Research*, *113*(F1 F01002). doi:10.1029/2007JF000769.

Owe, M., De Jeu, R. A. M., & Walker, J. P. (2001). A methodology for surface soil moisture and vegetation optical depth retrieval using the microwave polarization difference index. *IEEE Transactions on Geoscience and Remote Sensing*, *39*(8), 1643–1654.

Rüdiger, C., Calver, J. C., Gruhier, C., Holmes, T. R. H., De Jeu, R. A. M., & Wagner, W. E. (2009). An intercomparison of ERS-Scat and AMSR-E soil moisture observations with model simulations over France. *Journal of Hydrometeorology*, *10*(2), 431–447.

Shibata, A., Imaoka, K., & Koike, T. (2003). AMSR/AMSR-E Level 2 and 3 algorithm development and data validation plans of NASDA. *IEEE Transactions on Geoscience and Remote Sensing*, *41*(2), 195–203.

Teuling, A. J., Uijlenhoet, R., Hurkmans, R., Merlin, O., Panciera, R., Walker, J. P., & Troch, P. A. (2007). Dry-end surface soil moisture variability during NAFE06. *Geophysical Research Letters*, *34*, L17402 doi:10.1029/2007GL31001.

Ulaby, F. T., Moore, R. K., & Fung, A. K. (1981). *Microwave Remote Sensing: Active and Passive*. vol. 1. Norwood, MA: Artech House.

Wagner, W., Naeimi, V., Scipal, K., De Jeu, R. A. M., & Martínez-Fernández, J. (2007). Soil moisture from operational meteorological satellites. *Journal of Hydrology*, *15*, 121–131.

Walker, J. P., Grayson, R. B., Panciera, R., Zhan, X., & Houser, P. R. (2003). AMSR-E soil moisture validation efforts in the Australian arid zone. *American Geophysical Union, Fall Meeting Supplement*, *84*(46) Abstract H22E-05.

Walker, J. P., Merlin, O., Panciera, R., Kalma, J., Kim, E., & Hacker, J. (2006). *National airborne field experiments for soil moisture remote sensing. 30th Hydrology and Water Recourses Symposium, Tasmania* December 2006.

Wang, J. R. (1987). Microwave emission from smooth bare fields and soil moisture sampling depth. *IEEE Transactions on Geoscience and Remote Sensing*, *GE-25*(5), 616–622.

Wang, J. R., & Choudhury, B. J. (1981). Remote sensingo f soil moisture content over bare field at 1.4 GHz frequency. *Journal of Geophysical Research*, *86*, 5277–5282.

Wang, J. R., & Shcmugge, T. J. (1980). An empirical model for the complex dielectric permittivity of soils as a function of water content. *IEEE Transactions on Geoscience and Remote Sensing*, *18*, 288–295.

Wigneron, J. P., Kerr, Y., Waldteufel, P., Saleh, K., Escorihuela, M. J., Richaume, P., De Rosnay, P., Gurney, R., Calvet, J. C., Guglielmetti, M., Hornbuckle, B., Mätzler, C., Pellarin, T., & Schwank, M. (2007). L-band Microwave Emission of the Biosphere (L-MEB) model: description and calibration against experimental data sets over crop fields. *Remote Sensing of Environment*, *107*(4), 639–655.

Please cite this article as: Mladenova, I., et al., Validation of AMSR-E soil moisture using L-band airborne radiometer data from National Airborne Field Experiment 2006, *Remote Sensing of Environment* (2011), doi:10.1016/j.rse.2011.04.011